

Velocity jump in the crack propagation induced on a semi-crystalline polymer sheet by constant-speed stretching

Takako Tomizawa and Ko Okumura

Department of Physics, Ochanomizu University,
2-1-1, Otsuka, Bunkyo-ku, Tokyo, 112-8610, Japan

(Dated: April 9, 2019)

Abstract

It has long been known for elastomers that the velocity of crack propagation jumps as a function of strain. On the other hand, such a jump has not been reported in the literature for polymers which do not exhibit a rubbery plateau in the storage-modulus plot. Here, we report observation of jumps in crack propagation for semi-crystalline polymer sheets without the rubbery plateau, as a result of pulling the sheets at a constant speed. We discuss the advantages of this crack-propagation test under constant-speed stretching and provide physical interpretation of the velocity jump observed for non-elastomer sheets on the basis of a recently proposed theory for the velocity jump in crack propagation.

I. INTRODUCTION

Toughening of polymer materials is an important current problem. Tough polymers could even replace glass and metal used in automobiles to reduce their weight, which should greatly contribute to the reduction of energy consumption. For developing tough polymers, one of the relevant issues is the velocity-dependent properties of fracture and, in fact, this issue has been explored for various forms of polymers, which include adhesive [1–5], laminar [6] and viscoelastic polymers [7, 8], weakly cross-linked gels [9, 10], biopolymer gels [11], and biological composites [12].

In the rubber industry, the so-called pure shear test has long been performed for sheet samples of rubbers to estimate their toughness [13]. This test is performed in the following manner under a static boundary condition: (1) Firstly, a sheet is given a fixed strain through the top and bottom grips. (2) Secondly, the sheet is cut at one of the free side-edges with keeping the distance between the grips fixed. (3) Thirdly, the propagation speed of the crack is measured when it reaches a constant. (The constant speed is attained when the crack propagation length is long enough compared with the distance between the grips.) When this measurement is repeated numerous times at different given strains, the crack-propagation velocity is given as a function of the strain (or the energy release rate, which is identical to the fracture energy in this case).

It has long been known that the velocity of crack-propagation jumps as a function of the strain and that the jump is used to control toughness. This velocity jump observed in elastomers has actively been studied experimentally [14–17] and numerically [18]. Recently, an analytical model has been proposed to clarify the physical origin of the velocity jump [19], and the model is semi-quantitatively compared with experiments [20].

Although the velocity jump in the crack propagation under the static boundary condition is useful for evaluating toughness in developing new polymer-based materials in a sense that such a dangerous jump is better to be avoided for tough materials, the static crack-propagation test has been limited due to two factors: (1) No previous studies reported such jumps for resins other than elastomers. (2) Test requires numerous numbers of sample sheets and repetition of crack-propagation experiments to determine the velocity at jump.

In this study, we report the velocity jump for sheets of non-elastomer semi-crystalline polymers by performing crack-propagation test under a dynamic boundary condition, i.e.,

under constant-speed stretching, in which case the velocity at jump is determined by performing a single crack-propagation test. We demonstrate that this type of crack propagation test is much more sensitive to detect the jump and discuss the physical interpretation of the jump on the basis of the analytical theory [19]. Our study paves the way for a wide use of the velocity jump in developing tough polymer-based materials.

II. RESULTS AND DISCUSSIONS

A. Materials

In this study, we used sheets of a porous polypropylene provided by Mitsubishi Chemical Corporation. The thickness is $h = 23 \mu\text{m}$, the typical size of pore is of the order of submicrons to several microns (see Fig. 1 (a)), and the volume fraction is 0.44. The real and imaginary parts of the complex modulus are shown in Fig. 1 (b). The viscoelastic measurement is performed for a sample of width 4 mm and length 35 mm by giving a pre-stretching force of 0.2 N under a strain oscillation of amplitude 0.1 % with frequency 1 Hz. The melting point obtained by DSC performed under the temperature-increase rate $2^\circ\text{C}/\text{min}$. in the range from 30 to 200°C is 172°C (The endothermic peak corresponding to the melting of crystalline domains is relatively sharp). The crystalline degree of the polypropylene is approximately 54 per cent. This estimation is based on the melting enthalpy of the porous film $\Delta H = 112 \text{ J/g}$ and the equilibrium melting enthalpy of bulk polypropylene $\Delta H_0 = 209 \text{ J/g}$ ($\Delta H/\Delta H_0 = 0.54$). We show the stress relaxation curve in Fig. 1 (c), which suggests that the stress relaxes significantly within 30 minutes (see Sec. II D). In Fig. 1 (d), a result of the previous study [21] is shown for later convenience.

B. Stress-strain relation

The stress-strain relation shown in Fig. 2 (a) was measured at three different pulling speeds in the range from $U = 0.02 \text{ mm/s}$ to 0.4 mm/s . The measurements were performed for the sheet samples of width $W = 50 \text{ mm}$ and height $L = 125 \text{ mm}$ by clamping the top and bottom edge of the sample in a configuration similar to the one shown in Fig. 2 (b) but without the initial crack of length a . (See the text below for further details.) For

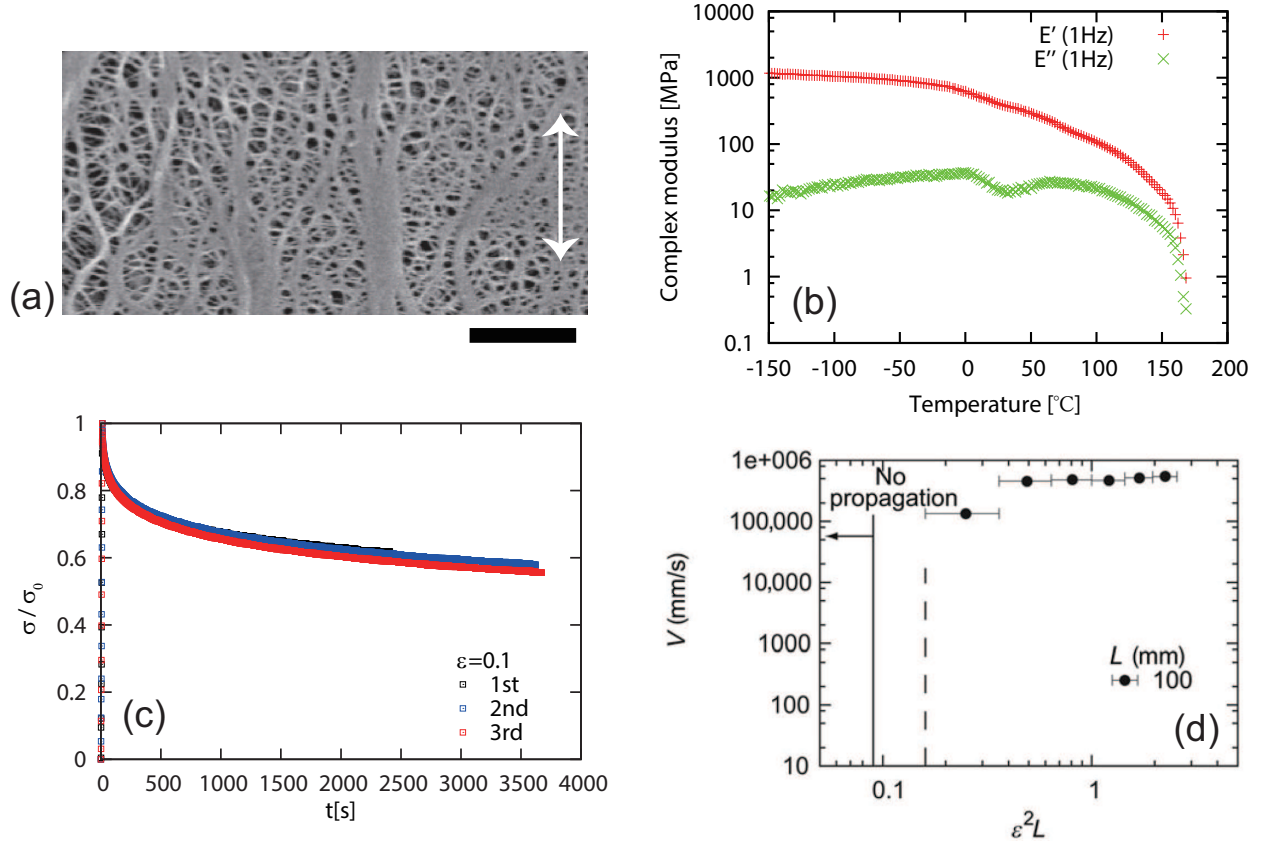


FIG. 1. (a) A SEM image of the porous polypropylene sheet used in the experiment. (b) Complex moduli as a function of temperature obtained at 1 Hz. (c) Stress relaxation curve obtained at the fixed strain of 0.1 for a sample of width 500 mm and of height $L = 100$ mm. The stress is renormalized by the maximum stress σ_0 . (d) Crack-propagation velocity vs. a measure of energy release rate $\epsilon^2 L$ under a fixed strain ϵ reported in the previous study [21]. (a) and (b): Copyright 2018 by Mitsubishi Chemical Corporation. (d) Reprinted from [21] (CC BY 4.0).

convenience, the stress is here defined as the force divided by the (initial) cross-section of the sheet sample Wh .

At each velocity U , three measurements were performed, which are well superposed with each other. However, the breaking point indicated by the symbol marks that abruptly drop from the smooth curves is weakly dependent on sample inhomogeneity. The breaking strain tends to be larger when U is small. The yielding stress is around 20-25 MPa and decreases with U , while the yielding stress around $\epsilon = 0.2$ is almost U -independent. These trends are intuitively natural, because as U becomes small polymer chains have longer time for

relaxation.

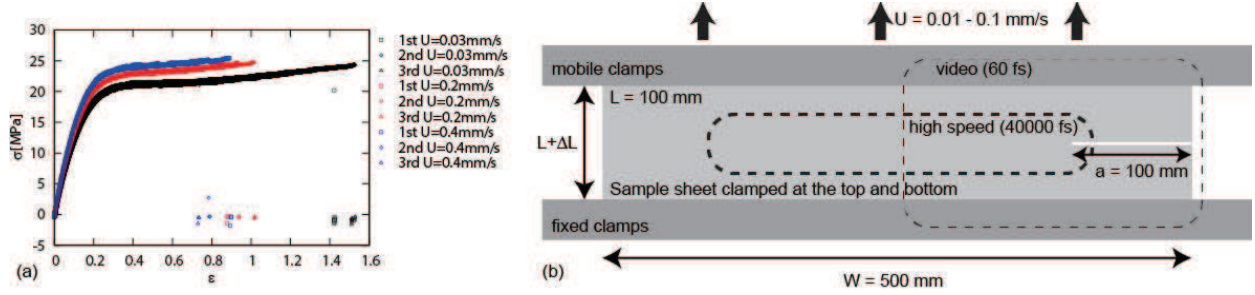


FIG. 2. (a) Stress vs. strain at three different pulling velocities. (b) Schematic illustration of the velocity jump experiment, where the areas covered by two cameras with different frame rates are indicated.

C. Crack-propagation test under a constant-speed stretching

The experiment is schematically explained in Fig. 2 (b). We clamped the top and bottom edges of a sample sheet of width $W = 500$ mm and of initial height $L = 100$ mm and introduced an initial crack of length $a = 100$ mm at one of the side edges. We then observed crack propagation from the initially introduced crack tip to the other side edge with pulling the top clamps at a fixed speed U in the range from 0.01 - 0.1 mm/s. The movement of the clamps is controlled by a slider system (EZSM6D040 K, Oriental Motor). The quantity ΔL is the increase in the height at each moment after stretching starts.

As a result, we found that the crack-propagation velocity jumps dramatically at a certain point. To analyze the dynamics before and after the jump, we set two cameras with significantly different frame rates. To capture the dynamics before the jump, we used a digital camera with a video function (D800E, Nikon) and acquired snapshots with the rate of 60 fps. For the dynamics after the jump, we used a high-speed camera (FASTCAM Mini UX100, Photron) with a lens (AF-S NIKKOR 20mm 1:1.8G ED, Nikon). The areas covered by the two cameras are indicated in Fig. 2 (b). The snapshot obtained with the 60-fps camera just after the jump records the moment after the crack reaches the opposite sample end. On the contrary, before the jump, no movements of the crack tip are recorded by the 40000-fps camera because of the limited memory storage of the high-speed camera.

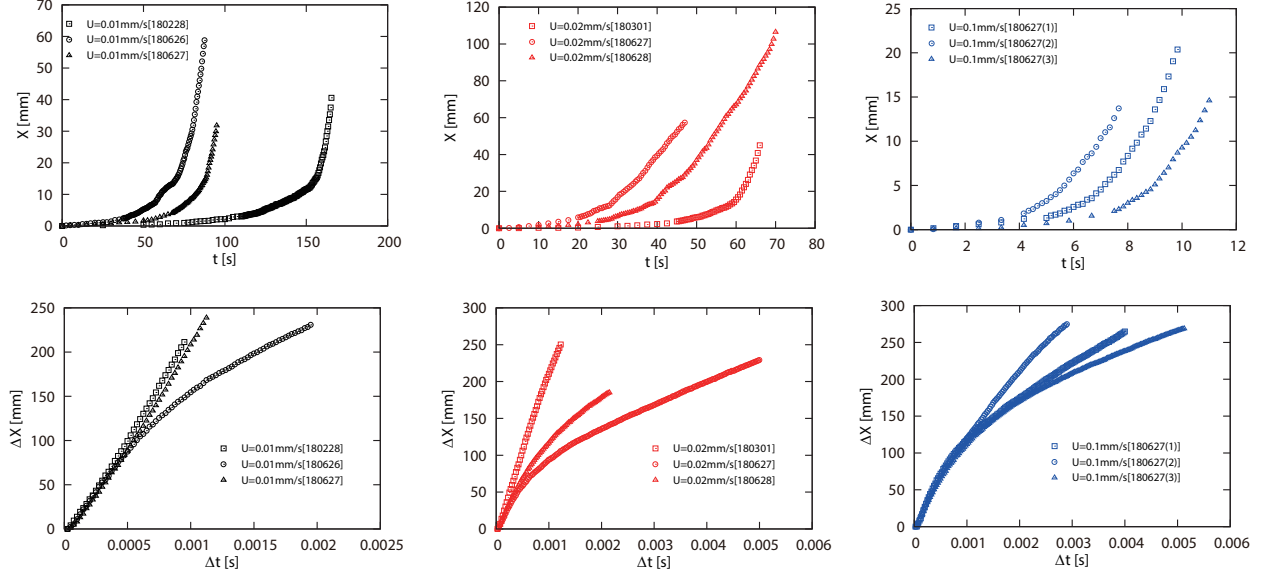


FIG. 3. Crack-tip position as a function of elapsed time at three different stretching velocities U . (Top) Results obtained from a 60-fps camera before the velocity jump. The position $X = 0$ and the time $t = 0$ correspond the tip position of the initial crack and the starting time of stretching, respectively. (Bottom) Results obtained from a 40000-fps camera after the velocity jump. The position $\Delta X = 0$ and the time $\Delta t = 0$ correspond the crack-tip position and the moment at the jump, respectively.

In the following, we explain the results shown in Figure 3. The data shown in the figure seem to exhibit strong sample dependence. However, considering experimental artifacts (difficulty in determining the stress-zero state in the case of Fig. 3(a) and an edge effect in the case of Fig. 3 (b)), sample dependence is in fact less strong than its appearance, as explained below. This is reasonable considering that bulk properties characterized in Fig 1 and Fig 2 by the rheology measurements and the stress-strain curve do not show strong sample dependence, although, in principle, the local distribution of pore size could affect the crack propagation.

The three graphs in the top panel of Fig. 3 show the results for the dynamics before the jump obtained by the 60-fps camera at different stretching velocities U . We see that there is a rather strong sample dependence. However, the dependence might be enhanced because of the difficulty in determining the zero-strain state, which corresponds to $t = 0$. For example, at $U = 0.1$ mm/s, the three plots are well superposed with each other if we allow time-shifts

of the order of a few seconds, which implies that the sample dependence is in fact relatively small. This order of time-shifts suggests a rough estimate for the magnitude of error in the increase in height ΔL , which is about 0.1 mm (i.e., U times a few seconds). This corresponds to the error in the strain $\simeq 0.001$ because $L = 100$ mm. Similar estimates for the errors in ΔL and the strain are obtained from the two remaining values of U . For example, at $U = 0.01$ mm, the time-shifts of 10 seconds would decrease the sample dependence significantly (i.e., it would make the three plots well superposed).

The three graphs shown in the bottom panel of Fig. 3 show the results for the dynamics after the jump obtained by the 40000-fps camera at different stretching velocities U . Just after the jump, the sample dependence of the data is fairly small. On the contrary, the speed (the slope) tends to decrease as the crack tip approaches the side edge opposite to the one at which the initial crack is introduced. Such a decrease in velocity would not be observed if the sample is long enough in the direction of crack propagation. This is called the edge effect and we try to avoid this effect in our velocity analysis presented below. (Since a slight error in identifying the zero-strain state leads to a significant difference in the position of the jump, apparent sample dependence due to the edge effect will be enhanced compared with real sample dependence.)

The crack-propagation velocity obtained from the data shown in Fig. 3 is given in Fig. 4. The velocity before the jump is obtained from the data shown in the top panel of Fig. 3. (The i th velocity V_i is obtained as the backward difference $V_i = (X_i - X_{i-1})/\delta t$ (with $\delta t = 1/60$ sec) from the smoothed i th position X_i given as $(x_i + x_{i-1} + \dots + x_{i-4})/5$ where x_j is the j th position of the raw data.) The velocity after the jump is obtained from the data shown in the bottom panel of Fig. 3 by using the initial region in which the sample dependence is small to avoid the edge effect. (The velocity is obtained as the forward difference $V_i = (x_i - x_{i+1})/\delta t$ (with $\delta t = 1/40000$ sec) of the raw $\Delta X - \Delta t$ data in the ranges $\Delta t = 0$ to 0.4 ms and $\Delta t = 0$ to 0.2 ms for $U = 0.01$ and 0.1 m/s and for $U = 0.02$ m/s, respectively.)

Although there exists the sample dependence probably originating from inhomogeneous porous structures, which tends to be enhanced because of experimental artifacts, some robust features are visible in Fig. 4. (1) The velocity changes nearly four orders of magnitude at the jump. (2) Before the jump the crack-propagation velocity is in the range around from 0.0001 to 0.01 m/s, which corresponds to the strain-rate range from 0.001 to 0.1 s^{-1} . (3) After the

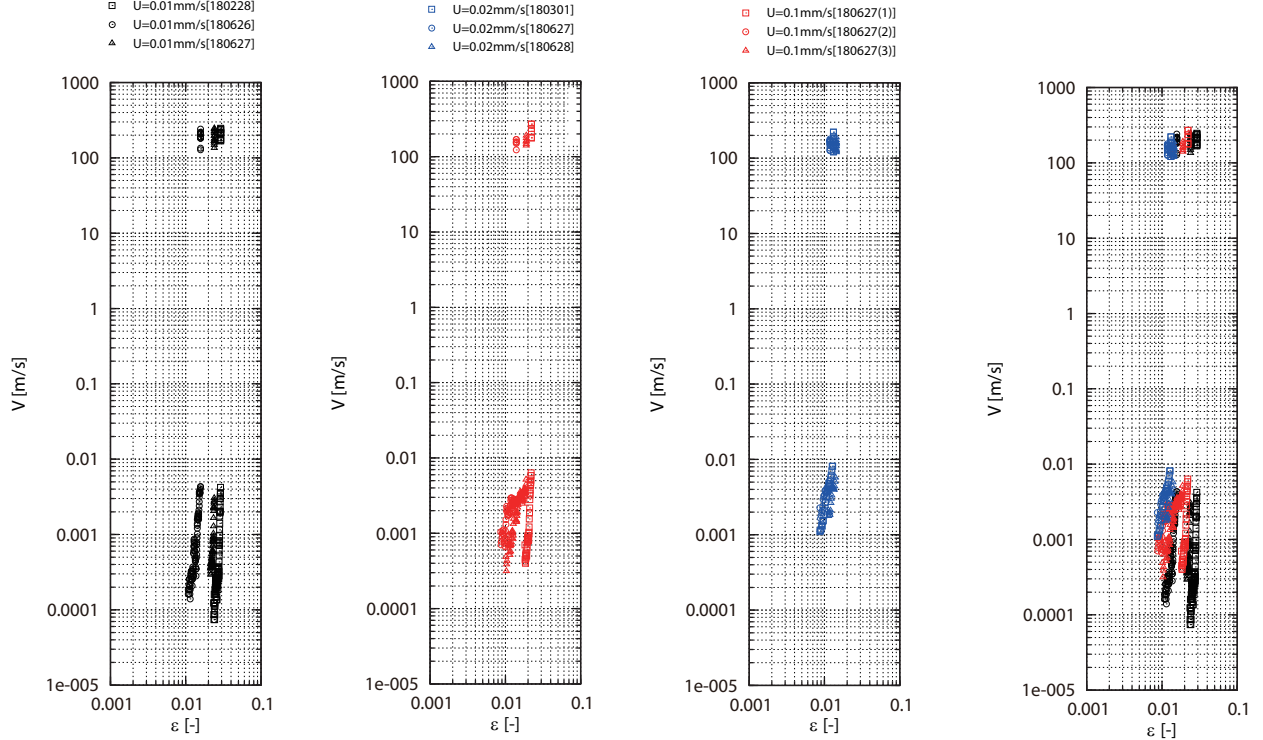


FIG. 4. Crack-propagation velocity vs strain at three different stretching velocity.

jump, the velocity reaches around a few hundreds m/s. (4) The strain at the jump tends to decrease as the pulling velocity U increases. (5) Before the jump, the crack-propagating velocity V as a function of ε is significantly large for high U . (6) After the jump, V tends to be small for high U and V seems to be on a straight line as a function of ε on the log-log plot. (7) The size of the jump tends to decrease as U increases.

The strain range for the data in Fig. 4 is around 0.01 to 0.04. In the corresponding strain range, the stress-strain relation is practically linear and free from the effect of plastic flow as seen in Fig. 2(a). This implies that the strain ε and fracture energy G (i.e., energy release rate) satisfy a simple linear relation on a log-log scale ($\log G = \text{const.} + 2 \log \varepsilon$). Accordingly, we here used the strain ε (instead of fracture energy G) for the horizontal axis.

D. Crack propagation test under a fixed-grip condition

We now discuss the previous results shown in Fig. 1 (c) [21], which is obtained by observing a constant-velocity crack propagation under a fixed strain. By repeating crack-

propagation experiments with changing the value of the fixed strain, one obtains the crack-propagation velocity as a function of the given strain. (We need at least one sample sheet to obtain a single point on the $V - \varepsilon$ plot.) Here, the velocity is given as a quantity $\varepsilon^2 L$, where L is the height of the sample. This quantity is proportional to the so-called energy release rate and the velocity is expected to be a universal function of this quantity for a certain material although L are different. The experimental geometry is similar to the one given in Fig. 2 (b). The differences are that the mobile pair of clamp is fixed to give a certain value of ΔL and that the small initiating crack is introduced at one of the side edges after ΔL is given. We note here for later convenience that this process of preparation, i.e., giving a fixed strain to the sheet before introducing a small cut to initiate crack propagation, requires a finite amount of time.

In this previous experiment, we failed to observe the velocity jump. Instead, we found that the crack propagates nearly at a constant speed around 500 m/s for ε larger than around 0.07 ($\varepsilon^2 L \simeq 0.5$) and that the crack does not propagate at all for ε smaller than around 0.03 ($\varepsilon^2 L \simeq 0.1$).

E. Comparison of the results under the dynamic and static boundary conditions

We find clearly that the velocity jump is observed in the present experiment performed under the dynamic boundary condition, whereas the jump is not observed in the previous experiment performed under the static condition. The high-velocity regime after the jump in the present study is fairly consistent with the high-speed crack propagation observed in the previous study. (In the present study the high-velocity regime after the jump is "short," i.e., observed in a small strain range at a given U . This does not suggest difference but is merely because the sample length is not enough: after the jump, the crack soon reaches the opposite side end of the sample.) However, the low-velocity regime before the jump in the present study is absent in the previous study, which marks the significant difference between the two experiments.

We consider the principal reason for not observing this regime under the static boundary condition is that the stress relaxation occurred in the above-mentioned preparation time for the fixed-grip experiment. In the previous experiment, the preparation time was of the order of 30 minutes, during which the stress is significantly relaxed (because this material

is a linear viscoelastic material for small strains) as suggested in Fig. 1 (c) to suppress the crack propagation. On the contrary, when the given strain is relatively high, because this material exhibits yielding behavior (see Fig. 2 (a)), the induced plastic deformation tends to suppress relaxation, and thus the crack-propagation behavior under the static condition becomes similar to that under the dynamic condition.

Note that under the dynamic boundary condition in the present study, there is no preparation time and the effect of stress relaxation is practically suppressed. By definition, the preparation time is the time duration from the moment one starts to give a fixed strain to the sample to the moment one introduces a cut at one of the free side edges after one finished giving the fixed strain. In the experiment under the dynamic boundary condition, crack keeps propagating with the given strain simultaneously increasing. This means that the dynamic test is free from preparation time and the effect of stress relaxation (during the preparation time) is by definition absent in the dynamic test.

F. Plausible physical pictures emerging from the previous theory

In our previous study [19], we showed that the glass transition that occurs near the very localized vicinity of the crack tip can trigger the velocity jump. This theory suggests that the velocity jump could be observed if the storage modulus possesses the glassy regime in the high frequency range and the rubbery regime in the low frequency range. The high-velocity regime after the jump reflects the glassy dynamics, whereas the low-velocity regime before the jump corresponds to the rubbery dynamics.

We consider the velocity jump observed in the present study is understood on the basis of this previous theory. As shown in Fig. 1 (c), this material clearly has the glassy regime and shows the glass transition temperature around at 0 °C. But, it starts to melt around at 170 °C, showing no rubbery plateau (or before showing the rubbery plateau). This implies that we cannot access the rubbery regime of this material by raising temperature. However, on the basis of the time-temperature correspondence, we may access the rubbery regime by increasing the time scale without facing melting of the sample, which we consider is realized by the present crack-propagation experiment. Because of the slow dynamics induced by the slow crack propagation, the material near the crack starts to behave like a rubber. This is our physical interpretation of the slow-velocity regime before the velocity jump. In other

words, the present result is consistent with and even expected from the previous theory, if we assume that our previous theory is applicable to the present case.

G. Advantages of the dynamic crack-propagation test

We here discuss the advantages of the dynamic crack-propagation test. As seen above, the dynamic test could be much sensitive to the velocity jump because it is less subject to the effect of strain relaxation. In addition, the velocity at the jump at each pulling velocity U is precisely detected because the strain value is dynamically and continuously changed with time. In other words, a fine tuning of strain is possible to obtain the precise value of strain at the jump. An important practical advantage is that the dynamic test is much more timesaving and needs much less amount of samples. This is because in the case of the static test we need one sample to obtain a single point on the velocity-strain plot. On the contrary, one entire curve for the velocity-strain relation is obtained from a single sample sheet. Note, however, that, as already mentioned, the dynamic test may not be practical if one would like to obtain the high-velocity regime over a wide range: we would need to have nearly an infinite sample width W in order to obtain a wide range of the high velocity range in the dynamic test.

H. Comparison of our results with results obtained from rubbers

We here compare our results with results obtained from rubbers. In the case of rubber, the velocity jump occurs typically from 10^{-1} mm/s to 1 m/s at a critical energy release rate. The ratio of the velocity just after the jump V_a to the velocity just before the jump V_b is about 10^4 , which is comparable to the value obtained the present case. As for V_a and V_b , both are about 100 times as large as those of rubbers. According to the previous theory [19], V_a and V_b both scale with the factor l/τ_R , i.e., the length scale l below which the continuum description breaks down divided by the characteristic time τ_R for the rubbery regime (see Eq. (16) and (17) in [20]). Compared with rubbers, τ_R tends to be larger because the plots of the complex elastic moduli tend to be shifted in the high temperature side in the present case. However, the length l may be much larger in the present case because of the porous structure, which may explain at least qualitatively why V_a and V_b are shifted to the higher

side.

In the slow mode regime, in which the propagation velocity V is smaller than V_b , the velocity V seems to scale with some power of the fracture energy G ($\sim \varepsilon^2$ in the present case) as in the case of rubbers: the plot V vs G (or ε) on a log-log scale is on a straight line. However, the slope of the straight line is much larger in the present case. This tendency is qualitatively in accord with the experimentally known fact (for rubbers) that the slope becomes large with the characteristic length scale l (i.e., cross-linking distance) [15]. As stressed above, l is expected to be much larger in the present case and, thus, from the experimentally known fact, the slope on a log-log scale in the slow mode regime is expected to be very large, which is supported by Fig. 4.

As for the fast mode, in which V is larger than V_a , comparison is generally difficult. This is because as explained in Sec. II E below, the crack propagation experiment under the dynamic boundary condition as in the present case, it is difficult to obtain the data in the fast mode regime in a wide range because of the limitation of the sample length (after the jump V is extremely fast).

III. CONCLUSION

We observed a jump in the crack-propagation speed as a function of applied strain for a polymer sheet which is not elastomer, i.e., whose storage modulus does not exhibit the rubbery plateau. The jump was not observed in the previous study in which the experiment is done under the static boundary condition. In the present study, by employing the dynamic boundary condition, we succeeded in observing the jump. The dynamic test demonstrated in the present study is promising because of a number of advantages such as the sensitivity to the velocity jump, timesaving and cost-effective features. If we assume that the previous theory [19] is applicable to the present results, plausible physical pictures emerge: (1) The velocity jump in the present study results from the glass transition that occurs in the vicinity of the crack tip. (2) The low-velocity regime before the jump may probe into the rubbery dynamics, which is usually hidden by melting and cannot be accessible by raising temperature.

ACKNOWLEDGEMENTS

The authors thank Dr. K. Tsunoda (Bridgestone) for discussion on the crack-propagation test under a constant pulling speed. They are grateful to Mitsubishi Chemical Corporation for providing sample sheets, the SEM image [Fig. 1 (a)], and the viscoelastic plots [Fig. 1 (b)], together with the results concerning the melting temperature and degree of crystallization of the sample. This work was partly supported by ImPACT program of Council for Science, Technology and Innovation (Cabinet Office, Government of Japan).

REFERENCES

- [1] AN Gent and J Schultz. Effect of wetting liquids on the strength of adhesion of viscoelastic material. *The Journal of Adhesion*, 3(4):281–294, 1972.
- [2] Manoj K Chaudhury. Rate-dependent fracture at adhesive interface. *The Journal of Physical Chemistry B*, 103(31):6562–6566, 1999.
- [3] Yoshihiro Morishita, Hiroshi Morita, Daisaku Kaneko, and Masao Doi. Contact dynamics in the adhesion process between spherical polydimethylsiloxane rubber and glass substrate. *Langmuir*, 24(24):14059–14065, 2008.
- [4] Costantino Creton, Edward Kramer, Hugh Brown, and Chung-Yuen Hui. Adhesion and fracture of interfaces between immiscible polymers: from the molecular to the continuum scale. *Adv. Polymer Sci.*, 156:53–136, 2002.
- [5] Satyam Bhuyan, François Tanguy, David Martina, Anke Lindner, Matteo Ciccotti, and Costantino Creton. Crack propagation at the interface between soft adhesives and model surfaces studied with a sticky wedge test. *Soft Matter*, 9(28):6515–6524, 2013.
- [6] AJ Kinloch, CC Lau, and JG Williams. The peeling of flexible laminates. *International Journal of Fracture*, 66(1):45–70, 1994.
- [7] JA Greenwood and KL Johnson. The mechanics of adhesion of viscoelastic solids. *Phil. Mag. A*, 43(3):697–711, 1981.

- [8] RA Schapery. A theory of crack initiation and growth in viscoelastic media. *International Journal of Fracture*, 11(1):141–159, 1975.
- [9] PG de Gennes. *C. R. Acad. Sci. Paris*, 307:1949, 1988.
- [10] F Saulnier, T Ondarcuhu, A Aradian, and E Raphaël. Adhesion between a viscoelastic material and a solid surface. *Macromolecules*, 37(3):1067–1075, 2004.
- [11] Maxime Lefranc and Elisabeth Bouchaud. Mode I fracture of a biopolymer gel: Rate-dependent dissipation and large deformations disentangled. *Extreme Mechanics Letters*, 1:97–103, 2014.
- [12] Eran Bouchbinder and Efim A Brener. Viscoelastic fracture of biological composites. *Journal of the Mechanics and Physics of Solids*, 59(11):2279–2293, 2011.
- [13] GJ Lake. Fracture mechanics and its application to failure in rubber articles. *Rubber Chem. Tech.*, 76(3):567–591, 2003.
- [14] A Kadir and AG Thomas. Tear behavior of rubbers over a wide range of rates. *Rubber Chem. Tech.*, 54(1):15–23, 1981.
- [15] K Tsunoda, JJC Busfield, CKL Davies, and AG Thomas. Effect of materials variables on the tear behaviour of a non-crystallising elastomer. *J. Mater. Sci.*, 35(20):5187–5198, 2000.
- [16] Yoshihiro Morishita, Katsuhiko Tsunoda, and Kenji Urayama. Velocity transition in the crack growth dynamics of filled elastomers: Contributions of nonlinear viscoelasticity. *Physical Review E*, 93(4):043001, 2016.
- [17] Yoshihiro Morishita, Katsuhiko Tsunoda, and Kenji Urayama. Crack-tip shape in the crack-growth rate transition of filled elastomers. *Polymer*, 108:230–241, 2017.
- [18] Atsushi Kubo and Yoshitaka Umeno. Velocity mode transition of dynamic crack propagation in hyperviscoelastic materials: A continuum model study. *Scientific Reports*, 7:42305, 2017.
- [19] Naoyuki Sakumichi and Ko Okumura. Exactly solvable model for a velocity jump observed in crack propagation in viscoelastic solids. *Scientific Reports*, 7(1):8065, 2017.
- [20] Ko Okumura. Velocity jumps in crack propagation in elastomers: Relevance of a recent model to experiments. *Journal of the Physical Society of Japan*, 87(12):125003, 2018.
- [21] Atsushi Takei and Ko Okumura. Crack propagation in porous polymer sheets with different pore sizes. *MRS Communications*, pages 1–6, 2018; <http://dx.doi.org/10.1557/mrc.2018.222>.